

Supplementary Information for:

All-optical stochastic switching of magnetization texture Fe_3Sn_2 dipolar skyrmions

András Kovács^{1*†}, Jonathan Weber^{2,3*†}, Michalis Charilaou^{4*}, Deli Kong^{1,5}, Alexander Schröder³, Nikolai S. Kiselev⁶, István Kézsmárki⁷, Rafal E. Dunin-Borkowski¹, Amir H. Tavabi¹, Sascha Schäfer^{2,8}

† These authors contributed equally.

¹ Ernst Ruska-Centre for Microscopy and Spectroscopy with Electrons, Forschungszentrum Jülich, Jülich, 52425, Germany.

² Department of Physics, University of Regensburg, Regensburg, 93053, Germany.

³ Institute for Physics, University of Oldenburg, Oldenburg, 26129, Germany.

⁴ Department of Physics, University of Louisiana at Lafayette, Lafayette, Louisiana, 70504, USA.

⁵ Department of Materials Science and Engineering, Southern University of Science and Technology, Shenzhen, 518055, China.

⁶ Peter Grünberg Institute and Institute for Advanced Simulations, Forschungszentrum Jülich, Jülich, 52428, Germany.

⁷ Experimental Physics V, University of Augsburg, Augsburg, 86135, Germany.

⁸ Regensburg Center for Ultrafast Nanoscopy, University of Regensburg, Regensburg, 93040, Germany.

Content

Supplementary Methods

1. Description of the statistical analysis.
2. On the effect of an externally applied magnetic field.
3. Dependence on the optical pulse duration.
4. Optical absorption in the Fe_3Sn_2 specimen.

Supplementary Figures

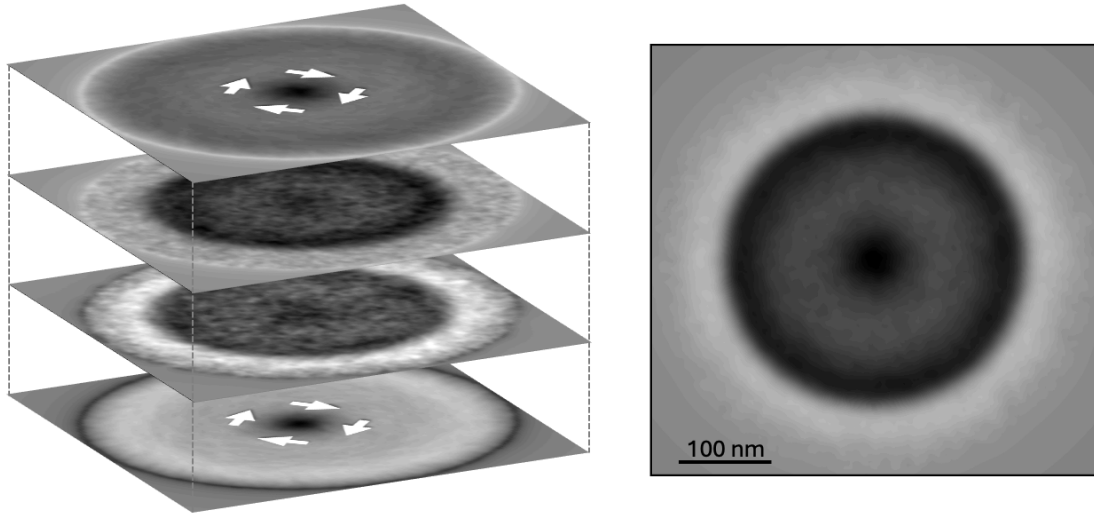
Figure 1. Simulated Lorentz contrast of dipolar skyrmions.

Figure 2. Analysis of the stochastic light-induced switching behavior of the Néel caps.

Figure 3. Statistical analysis of light-induced Néel cap switching behavior for varying excitation conditions.

Figure 4. Lorentz micrographs of the Fe_3Sn_2 lamella illuminated by 1-ps laser pulses.

Figure 5. Lorentz images of the *in situ* TEM heating experiment.

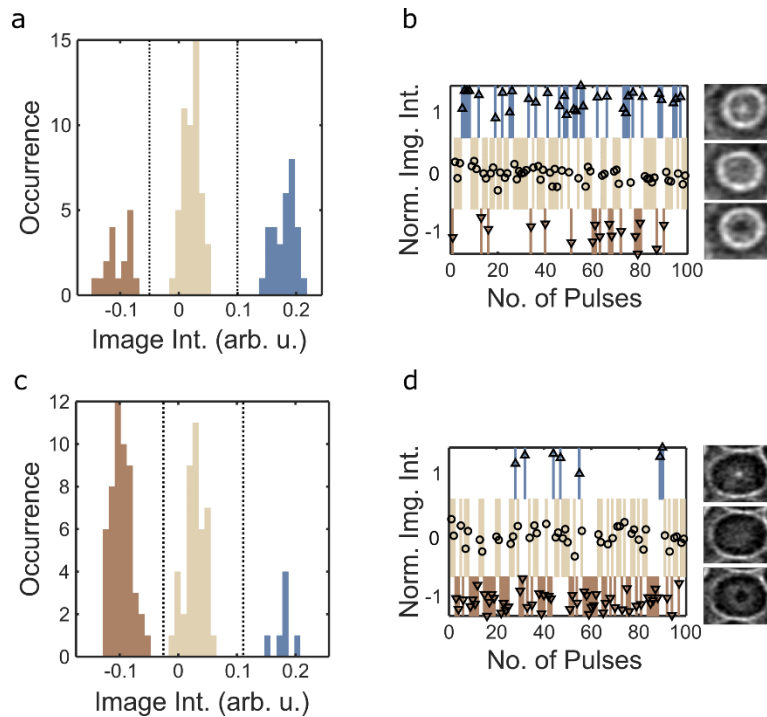


Supplementary Figure 1. Segmented phase shift image simulation of a dipolar skyrmion with matching field rotations of the Néel states, with opposed helicities as compared to Fig.1e in the main text, i.e. clockwise field rotations of its core Bloch and surface Néel states. The right panel shows the accumulated phase shift,

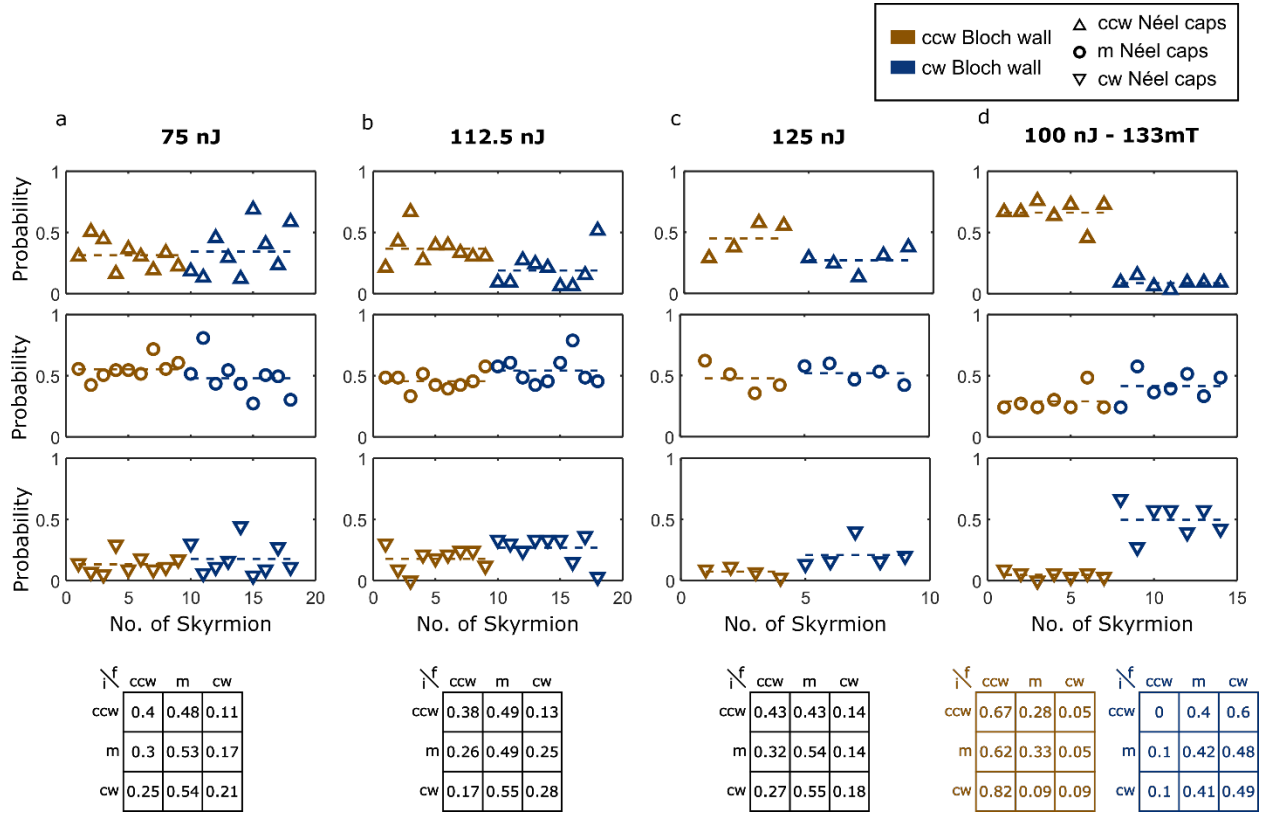
Method 1. Description of the statistical analysis

For the analysis of the magnetization state of the Néel caps in individual dipolar skyrmions, the Lorentz contrast in the recorded micrographs was analyzed. Between subsequent optical excitation events one to four Lorentz images were recorded, to allow for determination of the Néel cap state with a higher precision. MATLAB was used for all further evaluation steps, which include image binning (4 pixels x 4 pixels) and Gauss filtering (standard deviation of the two-dimensional Gaussian smoothing kernel of 2 pixels). To decrease the effect of diffraction contrast, which can change notably between consecutive optical pulse events obscuring the magnetization-induced contrast, Lorentz micrographs were high-pass Fourier filtered, excluding all spatial frequencies below $0.28 \mu\text{m}^{-1}$. Additionally, a low-pass Fourier filtering was applied, excluding all spatial frequencies above $16 \mu\text{m}^{-1}$. Slight variations of the position of individual dipolar skyrmions are taken into account by utilizing a built-in MATLAB function for circle detection in images based on a circular Hough transform implemented by the phase-coding method (Atherton 1999). Subsequently, the image intensity within a circular region in the center of the detected circle-object with a radius of three to seven pixels was extracted. The specific value was optimized for individual skyrmions, focusing on enhancing the distinction between the three contrast states (see histogram in Supplementary Fig. 2).

Categorization of the image intensity of the Néel caps of a specific dipolar skyrmion into one of the three possible contrast states was performed by introducing upper and lower thresholds. If the extracted image intensity within the central region of a dipolar skyrmion was above/below the upper/lower threshold value, the skyrmion was classified as being in the bright/dark state, corresponding to a counter-clockwise (ccw) or clockwise (cw) helicity of the two Néel caps. If the image intensity would fall between the threshold values, it was categorized as being in the mixed state, where the two Néel caps have opposing helicities. These threshold values were determined manually for each individual dipolar skyrmion, to account for the inhomogeneous background intensity in the Lorentz micrographs and are based on the minima of the image intensity distribution histograms as presented in Supplementary Fig. 2. If the threshold values could not be unambiguously defined, for instance when the histogram of the extracted image intensities did not show three distinct peaks, or when variations in background intensity were too extensive to ensure reliable results, the dipolar skyrmion was excluded from the analysis. The results of the analysis for varying excitation conditions are presented in Supplementary Fig. 3.



Supplementary Figure 2. Analysis of the stochastic light-induced switching behavior of the Néel caps magnetic state. (a & c) Histograms of the distribution of the image intensity within a circular region of two individual dipolar skyrmions. The according image intensity traces sorted for the number of incident optical pulses are presented in (b & c), the same as in Fig. 3 of the main text. The threshold values, utilized to distinguish between the bright-, mixed- and dark state are indicated as dotted lines in (a & c).



Supplementary Figure 3. Statistical analysis of light-induced Néel cap switching behavior for varying excitation conditions. Probability of the Néel cap to adopt the ccw/m/cw ($\Delta/o/\nabla$) state for a number of individual dipolar skyrmions upon excitation with a single light pulse with a pulse energy of (a) 75 nJ (incident fluence 10.6 mJ/cm²), (b) 112.5 nJ (15.5 mJ/cm²), (c) 125 nJ (17.7 mJ/cm²) and (d) 100 nJ (14 mJ/cm²) and an externally applied magnetic field of 133 mT. The optical focal spot size was increased to a 30 μ m diameter. At the bottom of each subfigure the probability matrices are presented, indicating the probability for a dipolar skyrmions with an initial Néel cap state (i) to adopt a final state (f) upon excitation with the indicated conditions. If an external magnetic field is applied (d) we observe a strong asymmetry between dipolar skyrmions with a ccw-Bloch domain wall (brown symbols) and those with a cw-Bloch domain wall (blue symbols), therefore the probability matrix is presented for both cases individually.

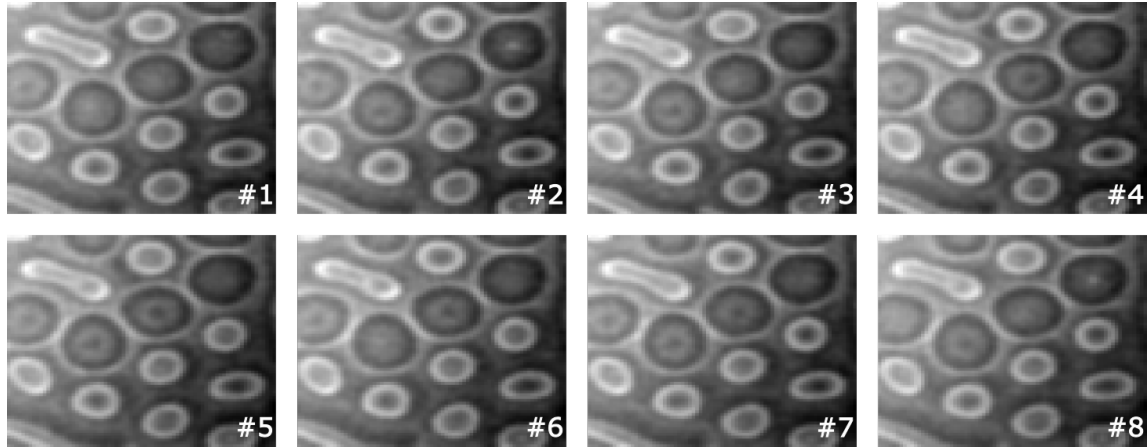
Method 2. On the effect of an externally applied magnetic field

Upon excitation of the Fe_3Sn_2 lamella with fs-optical pulses under an applied external magnetic field, utilizing the objective lens of the electron microscope, a qualitative change in the switching behavior is observed compared to experiments performed under magnetic remanence. In the absence of an external field, the probabilities of forming double-clockwise or double-counterclockwise surface cap helicities are approximately equal and appear independent of the helicity of the core Bloch wall. However, when a magnetic field of approximately 133 mT is applied, as shown in Supplementary Fig. 3d, a strong coupling between the Bloch wall helicity and the surface cap helicity emerges. This is in accordance with our expectations, as the degeneracy of helicity states observed in dipolar skyrmions in Fe_3Sn_2 is lifted in the presence of an external magnetic field, as previously reported (Kong 2024).

Method 3. Dependence on the optical pulse duration

To investigate the influence of the incident pulse duration on the switching dynamics, additional experiments were conducted using dispersively stretched optical pulses with a duration of approximately 1 ps (Supplementary Fig. 4). The qualitative characteristics of the light-induced switching process remained unchanged, and switching of the surface cap helicity state was still observed. However, the probability of observing a switching event per pulse was significantly reduced compared to experiments using femtosecond optical pulses. It remains unclear though, to what extent this reduction can be attributed solely to the increased pulse duration, or whether modifications in the spatial positioning of the optical focal spot, introduced by the stretching optics, also contribute. Further experimental investigation is required to disentangle these effects.

A certain pulse-length dependence of the switching rate would be expected for efficient electron-spin-coupling. Here, optical pulse durations below the electron-phonon coupling time of about 1 ps (Gonçalves-Faria 2024) would result in a temperature spike in the spin-system exceeding the lattice temperature attained after several picosecond. A finite contribution to the switching behavior of such non-equilibrium heating process therefore is apparent.



Supplementary Figure 4. Lorentz TEM micrographs showing the switching behavior upon pumping the Fe_3Sn_2 lamella by 1-ps laser pulses. The white number indicates the observed consecutive switching events.

Method 4. Optical absorption in the Fe_3Sn_2 specimen

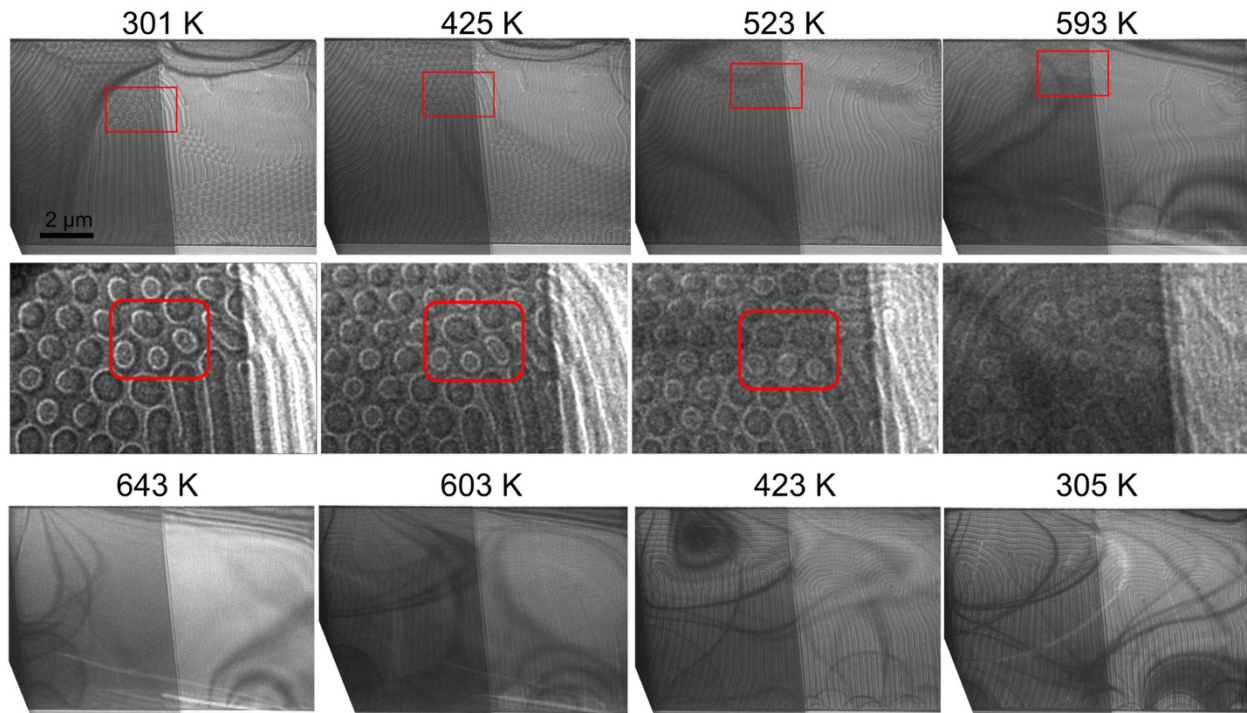
Based on experimental data and simulations reported in the Supplement of (Gonçalves-Faria 2024), we derive an optical conductivity for the Fe_3Sn_2 of $\sigma = 4.3 \times 10^5 \frac{1}{\Omega m}$ at 1.5 eV photon energy, which results in an optical absorption length of about 110 nm (neglecting the oblique incidence geometry and the optical anisotropy of the material). This would indicate an inhomogeneous excitation of the 200-nm thick lamella. However, the observation of switching events from double clockwise to double counter-clockwise surface cap helicities induced by a single optical pulse indicates that an excitation threshold is surpassed both on the illuminated top but also the bottom surface. Notably, once this threshold is exceeded, further increases in absorbed fluence appear to have no significant effect on the switching behavior.

The observation of a more homogeneous response across the film thickness could be explained by energy redistribution mechanisms, such as electron transport on femtosecond timescales or phonon transport on picosecond timescales.

Regarding the wavelength dependence, we expect only minor variations in the visible range, as the in-plane optical conductivity σ is rather unstructured for photon energies between 0.25-1.8 eV (Gonçalves-Faria 2024).

Furthermore, considering that the optical conductivity is dominated by its real part, the reflectivity for p-polarized 800-nm light at an incidence angle of 57° is obtained as 0.58, so that the absorbed fluence is about $F = 4.4 = 4.4 \text{ mJ/cm}^2$ for 100-nJ pulse energies (fluence

14.1 mJ/cm²). Based on reported molar heat capacity c_p (Gonçalves-Faria 2024), the corresponding temperature increase (after electron, phonon and spin equilibration) for a homogeneously optically heated, ~200 nm thick sample is obtained to be about $\Delta T = F \cdot M / (c_p \rho) = 86$ K (ρ : mass density, M : molar mass), demonstrating that the transient temperature becomes close to the Curie temperature.



Supplementary Figure 5. Lorentz images of Fe₃Sn₂ recorded at different temperatures showing the magnetic state changes near the Curie temperature. The experiment was carried out in magnetic remanence. Bubbles and dipolar skyrmions are eliminated at the Curie temperature and they did not form again upon cooling. The defocus value is 0.8 mm.

Bibliography

(Atherton 1999) T.J. Atherton, D.J. Kerbyson; *Size invariant circle detection*; Image and Vision Computing **17**; 11, 795-803 (1999)

(Kong 2024) L. Kong et al.; *Diverse helicities of dipolar skyrmions*, Phys. Rev. B. **109** 014401 (2024)

(Gonçalves-Faria 2024) M.V. Gonçalves-Faria et al.; *Coherent phonon and unconventional carriers in the magnetic kagome metal Fe₃Sn₂*, npj Quantum Mater. **9**, 31 (2024)